ACS APPLIED MATERIALS & INTERFACES

RESEARCH ARTICLE

www.acsami.org

Graft Copolymer-Templated Mesoporous TiO_2 Films Micropatterned with Poly(ethylene glycol) Hydrogel: Novel Platform for Highly Sensitive Protein Microarrays

Kyung Jin Son, Sung Hoon Ahn, Jong Hak Kim, and Won-Gun Koh*

Department of Chemical and Biomolecular Engineering, Yonsei University, 134 Sinchon-Dong, Seodaemoon-Gu, Seoul 120-749, Republic of Korea

ABSTRACT: In this study, we describe the use of organized mesoporous titanium oxide (TiO_2) films as three-dimensional templates for protein microarrays with enhanced protein loading capacity and detection sensitivity. Multilayered mesoporous TiO_2 films with high porosity and good connectivity were synthesized using a graft copolymer consisting of a poly(vinyl chloride) (PVC) backbone and poly(oxyethylene methacrylate) (POEM) side chains as a structure-directing template. The average pore size and thickness of the TiO_2 films were 50-70 nm and 1.5 μm, respectively. Proteins were covalently immobilized onto mesoporous TiO_2 film via 3-aminopropyltriethoxysilane (APTES), and protein loading onto TiO_2 films was about four times greater than on planar glass substrates, which consequently improved the protein activity. Micropatterned mesoporous TiO_2 substrates were prepared by fabricating poly(ethylene glycol) (PEG) hydrogel microstructures on TiO_2 films using photolithography. Because of nonadhesiveness of PEG hydrogel towards proteins, proteins were selectively immobilized onto surface-modified mesoporous TiO_2 region, creating protein microarray. Specific binding assay between streptavidin/biotin and between PSA/anti-PSA demonstrated that the mesoporous TiO_2-based protein microarrays yielded higher fluorescence signals and were more sensitive with lower detection limits than microarrays based on planar glass slides.

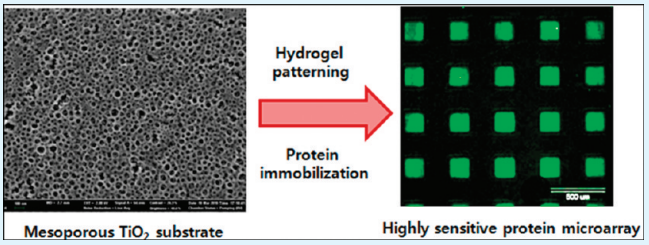

KEYWORDS: mesoporous titanium oxide (TiO_2) films, graft copolymer, poly(ethylene glycol) hydrogel microstructures, protein microarray

INTRODUCTION

Protein microarrays are important tools for high-throughput and large-scale bioassays. Protein-based assays such as antigen−antibody, enzyme−substrate reaction, and protein−protein interactions have greatly benefited from the distinct advantages of protein microarrays, which include small volumes of reagents and samples, fast reaction rates, reduced operating costs, and multiplexed detection.[1−5] Conventional protein microarrays consist of immobilized biomolecules that are spatially arranged on planar substrates such as glass and silicon through micropatterning techniques.[6−12] However, the amount of protein that can be immobilized to two-dimensional (2D) substrates is limited, leading to the generation of relatively weak analytical signals. Therefore, one of the major challenges in protein microarray technology is to develop appropriate substrates that are able to provide enhanced sensitivity and detection limits. The creation of (quasi) three-dimensional (3D) nanoarchitectures using nanomaterials and nanofabrication is a possible solution to achieve these goals, because 3D nanostructures offer larger surface areas that immobilize greater amounts of proteins than 2D substrates.[13] Two different strategies have been employed to create protein microarrays on nanoarchitectures. The first method is to use nano-sized molecules or materials that can be micropatterned onto conventional 2D substrates with immobilized proteins. For example, using micropatterned nanoparticles or dendrimers as substrates for protein immobilization improves the sensitivity of assays because they have curved structures with numerous functional groups that provide more space for protein attachment than planar surfaces.[14−17] The second method is to employ nanostructured substrates directly as protein host matrixes without guest nanomaterials. Nanoporous alumina or silicon, and electrospun nanofibers have previously been used as substrates for protein microarrays prepared by direct spotting.[18−20] Using nanostructured substrates enhances the sensitivity of protein microarrays, because 3D arrays increase protein binding capacity by immobilizing proteins throughout the thicknesses of the supporting materials.

Nanostructured titanium oxide (TiO_2) has recently emerged as a candidate biocompatible substrate due to attractive features such as good stability in aqueous media and optical transparency. Several groups have demonstrated the potential applications of nanostructured TiO_2 substrates for use in highly sensitive protein-based

Received: November 19, 2010
Accepted: January 17, 2011
Published: February 3, 2011

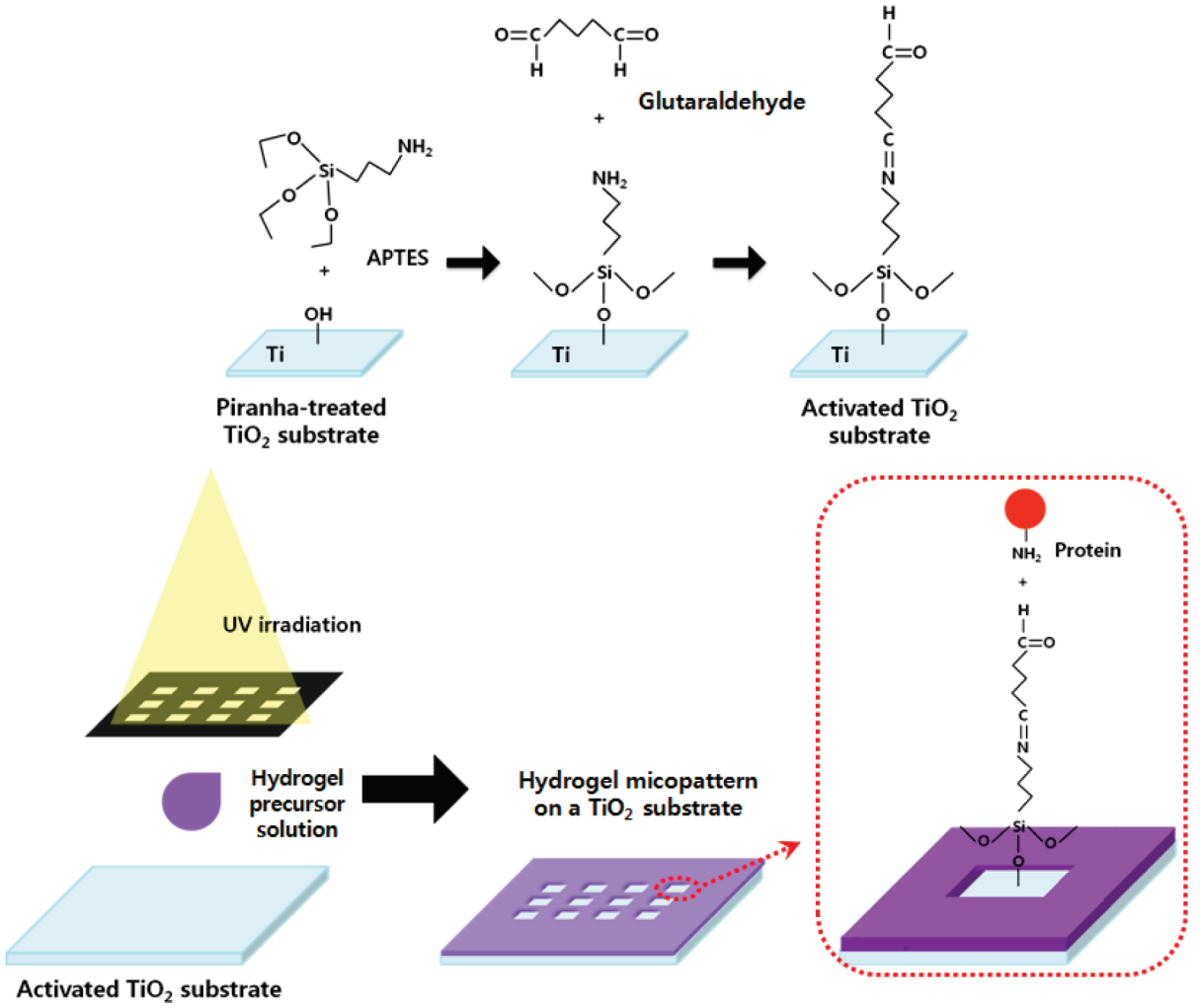

Figure 1. Schematics of preparing protein-immobilized mesoporous TiO_2 film that were micropatterned with PEG hydrogels.

assays, in which nanostructured TiO_2 substrates were prepared as macroporous inverse opal, nanotube, or nanoparticle-coated structures.[21−25] Other attractive features of TiO_2 substrates include their photocatalytic properties, which facilitate protein-based biosensor self-cleaning such that the substrates are reusable after UV exposure. Song et al. reported that several minutes of UV treatment allows protein-immobilized TiO_2 surfaces to return fully to their original conditions, and that repeated protein immobilization and immunoassays produced identical results even after ten use/reuse cycles.[26] Although previous studies have used nanostructured TiO_2 for the fabrication of protein microarrays, the use of multilayered and interconnected mesoporous TiO_2 films in protein microarrays has never been reported, to the best of our knowledge.

In this study, we utilized mesoporous TiO_2 to fabricate 3D substrates for protein microarrays for use in high-sensitivity bioassays. Organized mesoporous TiO_2 films were synthesized using a graft copolymer consisting of poly(vinyl chloride)(PVC) backbone and poly(oxyethylene methacrylate)(POEM) (PVC-g-POEM) as a structure directing agent. The surfaces of the resultant TiO_2 were modified to covalently immobilize protein, and micropatterned mesoporous substrates were prepared by incorporation of poly(ethylene glycol) (PEG) hydrogel microstructures into TiO_2 substrates. Because proteins do not adhere to PEG hydrogels, proteins are selectively immobilized onto surface-modified TiO_2 microdomains, facilitating the creation of protein microarrays. The protein-loading capacities and sensitivities of the resultant mesoporous TiO_2-based systems were compared with those of a corresponding planar substrate-based system.

EXPERIMENTAL SECTION

Materials. Poly(ethylene glycol) diacrylate (PEG-DA) (MW 575), o-dianisidine, 2-hydroxy-2-methylpropiophenone (HOMPP) (photoinitiator), glucose oxidase (GOX, from *Aspergillus niger* type II, 50 000 unit/g solid), peroxidase (POD, Type I, from horseradish, 80 units/mg of solid), β-D-glucose, 3-aminopropyltriethoxysilane (APTES), bovine serum albumin(BSA) and BSA conjugated with fluorescein isocyanate (FITC-BSA) were purchased from Sigma-Aldrich (Milwaukee, WI, USA). Glutaraldehyde (2.5% in solution) was purchased from Junsei Chemical (Tokyo, Japan). Biotinyl-3,6,9-dioxaoctanediamine (biotin-NH_2), prostate-specific antigen (PSA), anti-PSA antibody (anti-PSA) and a micro-BCA protein assay kit were obtained from Pierce (Rockford, IL,USA). FITC−labeled streptavidin (FTIC-STV) was purchased from Biosource (Camarillo, CA, USA). An Alexa Fluor 488 Monoclonal antibody labeling kit purchased from Invitrogen (Carlsbad, CA, USA) was used to label anti-PSA. A chrome sodalime photomask for photolithographic patterning of hydrogels was purchased from Advanced Reproductions (Andover, MA, USA). The phosphate buffered saline (PBS, 0.1 M, pH 7.4) used in all

dx.doi.org/10.1021/am101141z |*ACS Appl. Mater. Interfaces* 2011, 3, 573–581

experiments included 1.1 mM potassium phosphate monobasic, 3 mM sodium phosphate dibasic heptahydrate, and 0.15 M NaCl in deionized water.

Instruments. Photopolymerization of PEG-DA was performed using a 365 nm, 300 mW/cm^2 UV light source (EFOS Ultracure 100ss Plus, UV spot lamp, Mississauga, Ontario, Canada). Atomic force microscopy (AFM) measurements were performed on a Dimension 3100/Nanoscope Iva (Digital Instruments, Santa Barbara, CA, USA) in tapping mode. Surface modifications were monitored by X-ray photoelectron spectroscopy (XPS) (Kratos Analytical Inc., Chestnut Ridge, NY, USA), and solution absorbance was measured using a VersaMax tunable microplate reader (Molecular Devices, Sunnyvale, CA, USA). Scanning electron microscopy (SEM) was performed with a JEOL T330A at 15 kV (JEOL, Ltd., Tokyo, Japan) to observe pattern morphology. A Zeiss Axiovert 200 microscope equipped with an integrated color CCD camera (Carl Zeiss Inc., Thornwood, NY, USA) was used to obtain optical and fluorescence images. Image analyses were performed using commercially available image analysis software (KS 300, Carl Zeiss Inc.).

Fabrication of Mesoporous TiO_2 Substrate. Mesoporous TiO_2 substrates were prepared via a sol−gel process by templating amphiphilic PVC-g-POEM graft copolymer that was synthesized by previously reported method.[27] Briefly, the solution was prepared by slowly adding 0.28 g of HCl (37%) to 0.48 g of titanium(IV) isopropoxide (TTIP) in tetrahydrofuran (THF) under vigorous stirring. Separately, 0.1 g of amphiphilic PVC-g-POEM graft copolymer with PVC:POEM 4:6 weight ratio was dissolved in 2.9 g of THF and added to the TTIP/HCl/THF solution. The resulting solution was aged at ambient temperature with stirring for at least 3 h and spin-coated onto a glass slide (1500 rpm, 30 s). Upon calcination at 450 °C for 4 h, all organic chemicals including the graft copolymer were completely removed from the mesoporous TiO_2 films.

Protein Immobilization on the Mesoporous TiO_2 Substrate. Proteins were covalently immobilized on mesoporous TiO_2 substrates via reactions with APTES and subsequent activation with glutaraldehyde. First, TiO_2 substrates were immersed in piranha solution, consisting of a 3:1 ratio of 30% sulfuric acid and 30% hydrogen peroxide for 30 minutes at 80 °C, washed thoroughly with deionized water, and dried under nitrogen. Silanization with APTES was done by incubating TiO_2 substrates in a solution of 3% v/v APTES in 95% v/v ethanol under a nitrogen environment for 2 h at room temperature. The substrates were then flushed with ethanol to remove non-covalently bound APTES, and cured at 100 °C for 2 h. After APTES treatment, the substrates were immersed in a 2.5 % v/v solution of glutaraldehyde in PBS for 2 h at room temperature to activate the amine groups in APTES, and then incubated with target concentration of protein solution for 3 h. To serve as a reference, proteins were also immobilized on APTES-coated glass slides instead of TiO_2 substrates.

Calculation of Surface Density of Deposited BSA. After specific amount of BSA was reacted with a substrate in the incubation solution, the substrate was removed from the solution and the amount of BSA that remained in the solution was determined using a BCA standard working agent. The difference between initial and final amount of BSA was the amount BSA that was immobilized onto substrate. Finally, surface density was obtained by dividing the amount of immobilized BSA by apparent surface area of the substrate.

Activity Assays of Immobilized Enzymes. The activity of immobilized GOX was assessed by spectrophotometric determinations of the amounts of hydrogen peroxide that were formed, which is based on the oxidation of o-dianisidine through a peroxidase-coupled system.[28] For the GOX activity assay, 1.2 mL of 0.21 mM *o*-dianisidine solution, 0.25 mL of 5 mM β-D-glucose solution, and 0.05 mL of 2 mg/mL POD solution were added to 1.5 cm × 1.5 cm GOX-immobilized substrates and allowed to react for 1 h at 37 °C. The reaction was stopped with the addition of 1 mL of 2M hydrochloric acid, and the absorbance was measured at 405 nm in a microplate reader.

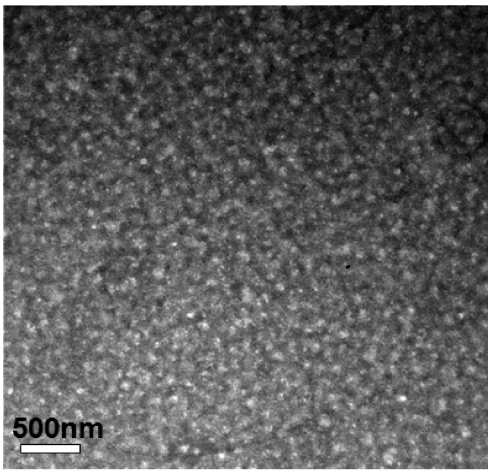

(a)

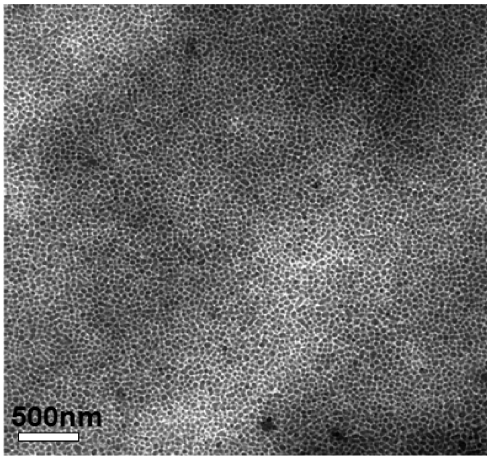

(b)

Figure 2. TEM images for PVC-*g*-POEM graft copolymer prepared from (a) THF solution and (b) THF/H_2O/HCl solution.

Fabrication of PEG Hydrogel Micropatterns on TiO_2 Substrates. PEG hydrogel micropatterns were fabricated using PEG-DA (MW 575) macromers. Precursor solution consisting of 1 mL of 50% v/v PEG-DA and 20 μL of HOMPP was dropped onto surface-modified mesoporous TiO_2 substrates and then exposed to UV light through a photomask for 0.2 seconds. After UV exposure, only the exposed precursor solution underwent free radical-induced crosslinking and became insoluble in common PEG solvents such as water. The desired hydrogel micropatterns were successfully obtained on mesoporous TiO_2 substrates by flushing the substrates with PBS. Finally, we incubated the micropatterned substrates with protein solution to produce protein microarrays. The experimental methods used to prepare protein microarrays on TiO_2 nanoporous substrates are summarized in Figure 1.

Assay of Streptavidin−Biotin Reaction. Hydrogel-micropatterned TiO_2 substrates were used to assess molecular recognition between biotin and streptavidin. A 10 mM solution of biotin-NH_2 in PBS was directly coupled to micropatterned TiO_2 substrates with surfaces that were modified using immobilization strategy described above. After the immobilization of biotin-NH_2 on the substrates, TiO_2 substrates were incubated with different concentrations of FITC-SA solution for 10 min. The binding of streptavidin to micropatterned biotin was visualized and quantified using fluorescence microscopy.

Detection of PSA. Micropatterned mesoporousTiO_2 substrates were reacted with a 20 ng/mL solution of anti-PSA in PBS for 2 h at

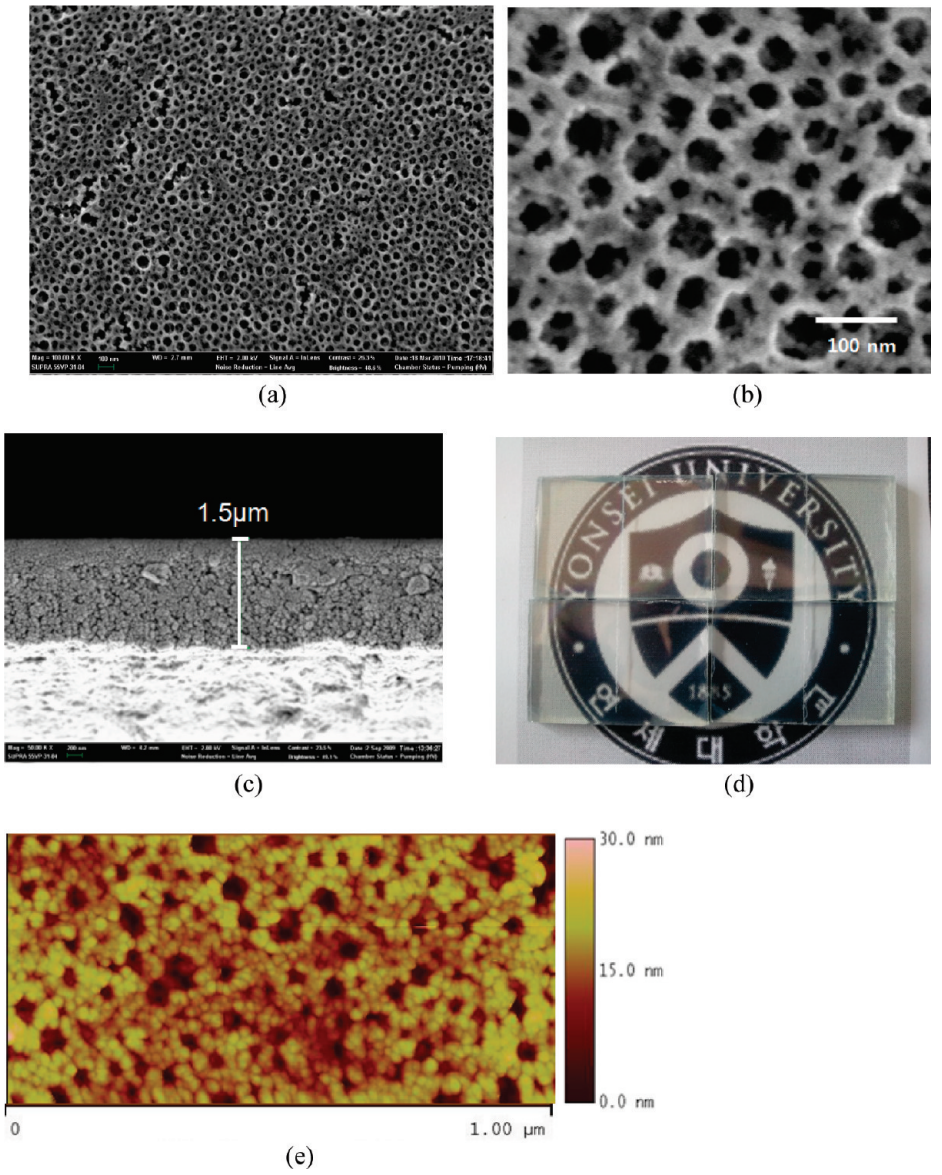

Figure 3. Multilayered mesoporous TiO_2 film fabricated on glass slide. (a) SEM image of mesoporous TiO_2 (top view), (b) highly magnified SEM image showing multilayered and interconnected mesoporous structures of TiO_2 film, (c) SEM image of cross-section of TiO_2 film, (d) photograph of the transparent TiO_2 films prepared on glass slides, (e) AFM image of mesoporous TiO_2 film.

room temperature. After immobilization of anti-PSA, TiO_2 substrates were blocked with BSA solution (1 wt % BSA in PBS solution) for 2 h, and subsequently reacted with different concentrations of PSA for 2 h at room temperature. To visualize immunoassays, we used sandwich immunoassays with fluorescence-labeled antibodies. We used the Alexa Fluor 488 Monoclonal antibody labeling kit, and labeled anti-PSA with Alexa 488 as described in the manufacturer's protocol.[29] After the reaction between anti-PSA and PSA, 20 ng/mL solution of fluorescence-labeled anti-PSA in PBS was introduced to the substrate surface and incubated for 2 h. The substrate was rinsed with PBS and dried under a nitrogen environment. The results of the immunoassay were visualized and quantified using fluorescence microscopy.

RESULTS AND DISCUSSION

Preparation of Mesoporous TiO_2 Substrate. Generally, organized mesoporous TiO_2 films have been synthesized via a sol-gel process using an amphiphilic block copolymer, because a microphase-separated structure into the hydrophilic and hydrophobic domains plays a crucial role for preparing organized mesoporous TiO_2 films.[30−33] In this study, instead of using block copolymer, we synthesized organized mesoporous TiO_2 films using a graft copolymer as a structure directing agent because a graft copolymer is more attractive than a block copolymer due to its lower cost and easier synthetic method. PVC-g-POEM graft copolymers showed randomly microphase-separated structure without regular patterns upon casting from tetrahydrofuran (THF) solution, which is a good solvent for both polymer chains (Figure 2a). Dark regions represent the hydrophobic domains of the PVC main chains, whereas bright regions indicate the hydrophilic POEM side chains. When small amounts of H_2O/HCl were introduced to control polymer-solvent interactions, organized micellar morphologies with 50−70 nm in diameter was obtained (Figures 2b). It is because the H_2O/HCl mixture is

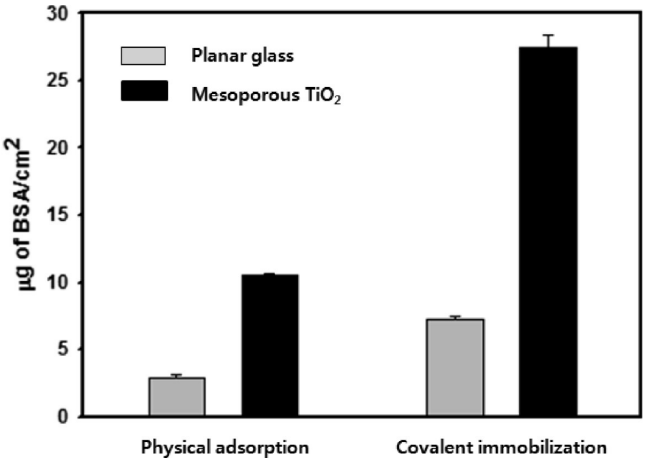

Figure 4. Amount of BSA immobilized on planar glass and mesoporous TiO_2. (BSA was immobilized onto substrates via physical adsorption and covalent bonding.

a poor solvent for PVC chains, resulting in decreases in swelling of PVC main chains and increases in stretching of POEM side chains.

The organized PVC-*g*-POEM graft copolymer with micellar morphology was templated to synthesize mesoporous TiO_2 films via a sol−gel process. As a result, organized, multilayered mesoporous TiO_2 films with high porosity and good connectivity were obtained as shown in Figure 3a and 3b. The mesoporous TiO_2 film (Figure 3a) exhibited good similarities with the organized PVC-*g*-POEM (Figure 2b) in terms of spatial distribution patterns, indicating the robust and precise structure-directing agent of the graft copolymer. Good miscibility and interactions between TTIP and POEM might allow TTIP to be selectively incorporated into hydrophilic POEM domains where TiO_2 crystallites are formed in situ during calcination. The mesoporous TiO_2 films were 1.5 μm thick and highly transparent, as shown in Figures 3c and 3d. The morphologies of mesoporous TiO_2 films were further confirmed by AFM as shown in Figure 3e. Calculations of effective surface area based on AFM revealed that TiO_2-coated substrates had larger surface areas than flat glass slides by 28.9 ± 8.1%. However, we believe the true increase of surface area is actually much greater than this value, because of the multilayered and interconnected mesoporous structure of TiO_2 films.

Immobilization of Proteins on TiO_2 Substrates. High-density of immobilized proteins on substrates enhances sensitivity and lowers the detection limits of protein-based biosensors. To investigate whether mesoporous TiO_2 substrates provide more space for protein loading due to increased surface area, the amounts of BSA immobilized on TiO_2 substrates were quantified and compared to those on planar glass slides. First, BSA was immobilized on unmodified TiO_2 substrates by physical adsorption. Although more BSA was immobilized onto TiO_2 substrates (10.543 ± 0.081 $\mu g/cm^2$) than on glass slides (2.848 ± 0.288 $\mu g/cm^2$) due to the larger surface areas of TiO_2 substrates as shown in Figure 4, weak attachment of BSA onto substrates resulted in significant leaching of BSA. In order to permanently immobilize proteins onto TiO_2 substrates and increase protein loading densities, the surfaces of TiO_2 substrates were modified to covalently immobilize proteins. APTES treatments were performed to supply amine groups that could serve as sites for protein immobilization. Using the glutaraldehyde reaction, we

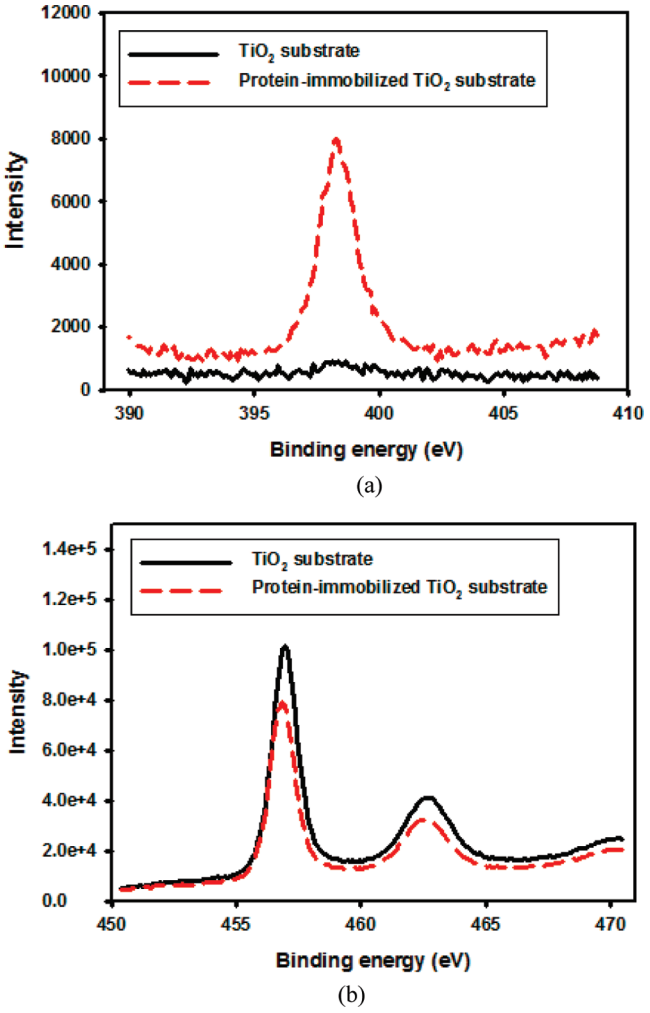

Figure 5. Narrow-scan XPS spectra of protein-immobilized and bare TiO_2 film: (a) N 1s and (b) Ti 2p peaks.

converted the amine groups in APTES to aldehyde groups that could react other amine groups in proteins to form stable imine linkages. The results shown in Figure 4 also indicate that surface modifications resulted in dramatic increases in the amount of BSA adhered to both mesoporous TiO_2 and planar glass substrates. However, mesoporous TiO_2 substrates possessed four-fold higher protein loading capacities than planar glass slides. Immobilization of BSA onto TiO_2 substrates was further characterized with XPS. Figure 5 shows XPS spectra for bare and BSA-immobilized TiO_2 substrates. As shown in Figure 5 (a), the XPS spectrum of a bare TiO_2 substrate did not contain an N 1s peak, whereas N1s signals are observed for a BSA-immobilized TiO_2 substrate due to the presence of peptide linkages in proteins. On the other hand, the Ti 2p peak decreased after the immobilization protein, suggesting that the TiO_2 surface was covered with BSA (Figure 5b).

Although improving protein-binding capacity is important for developing biosensors with better sensitivity, the real effectiveness of protein immobilization approaches is revealed in the activity of the immobilized proteins. Higher loading capacity does not always lead to higher activity, because steric interference between immobilized proteins can hinder access of target molecules. The activities of proteins immobilized on different surfaces were investigated using GOX as a model protein. Similar

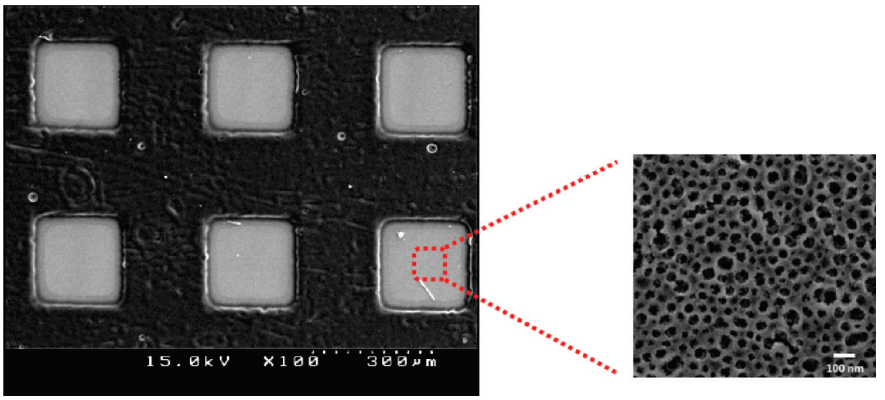

Figure 6. SEM image of microwells consisting of mesoporous TiO_2 bottom and PEG hydrogel walls.

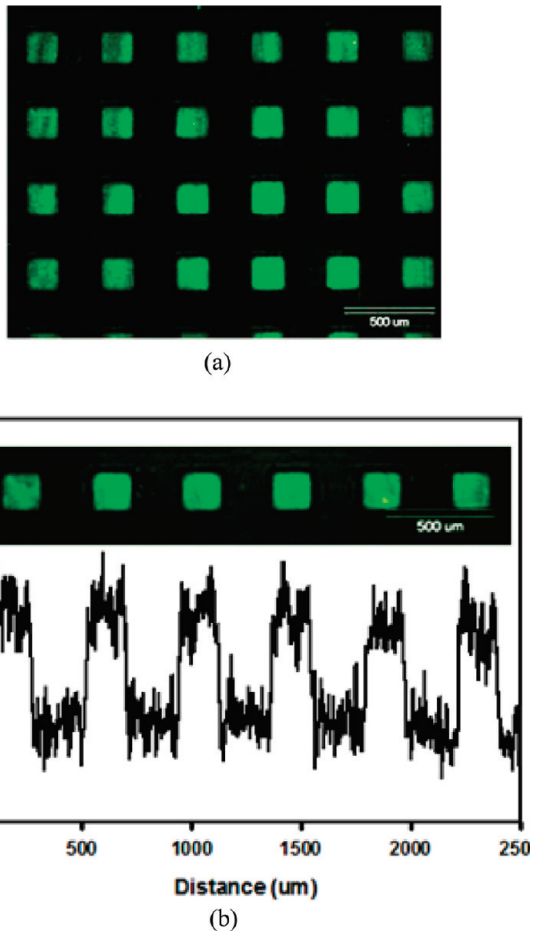

Figure 7. Immobilization of FITC-BSA on micropatterned TiO_2 substrates. (a) Fluorescence image of microwell array that were obtained after FITC-BSA was covalently immobilized onto activated TiO_2 regions, (b) fluorescence intensity profile across one row of microwell array immobilizing FITC-BSA.

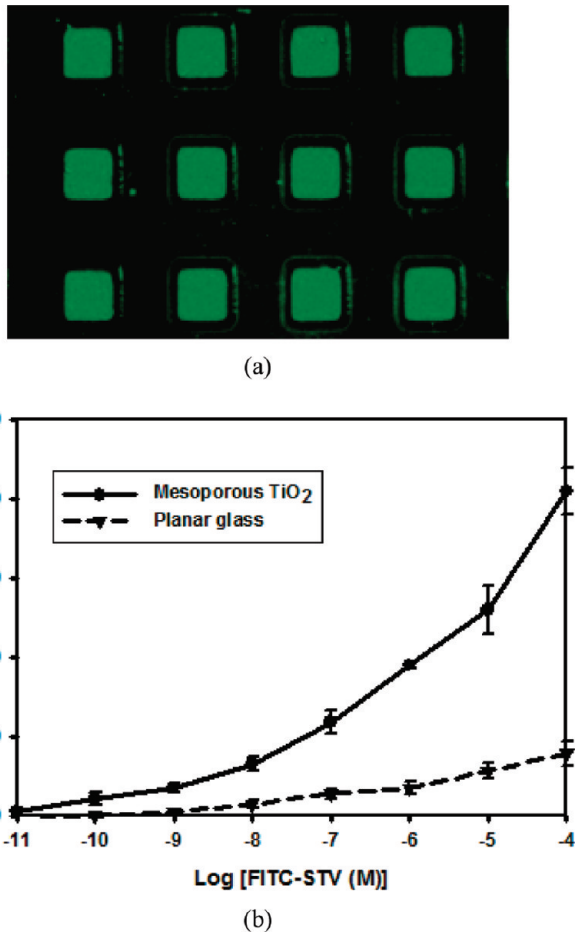

Figure 8. Biotin−Streptavidin assay on the micropatterned TiO_2 substrate: (a) Fluorescence image of FITC-STV bound to micropatterned biotin, (b) relationship between concentration of FITC- STV and the fluorescence intensity.

to the results of experiments assessing protein-binding capacity shown in Figure 4, covalent immobilization and mesoporous TiO_2 substrate led to higher activity than physical immobilization and planar glass substrate, respectively. Consequently, mesoporous TiO_2 substrates that covalently immobilized GOX showed the highest activities.

Preparation of Micropatterned Mesoporous TiO_2 Substrates. Hydrogel micropatterns were fabricated on surface-modified mesoporous TiO_2 substrates by taking advantage of the abilities of PEG-DA to turn into crosslinked hydrogel upon exposure to UV light and to create negative patterns via photolithography. When PEG hydrogel micropatterns were prepared on bare silicon or glass substrates, the hydrogel micropatterns

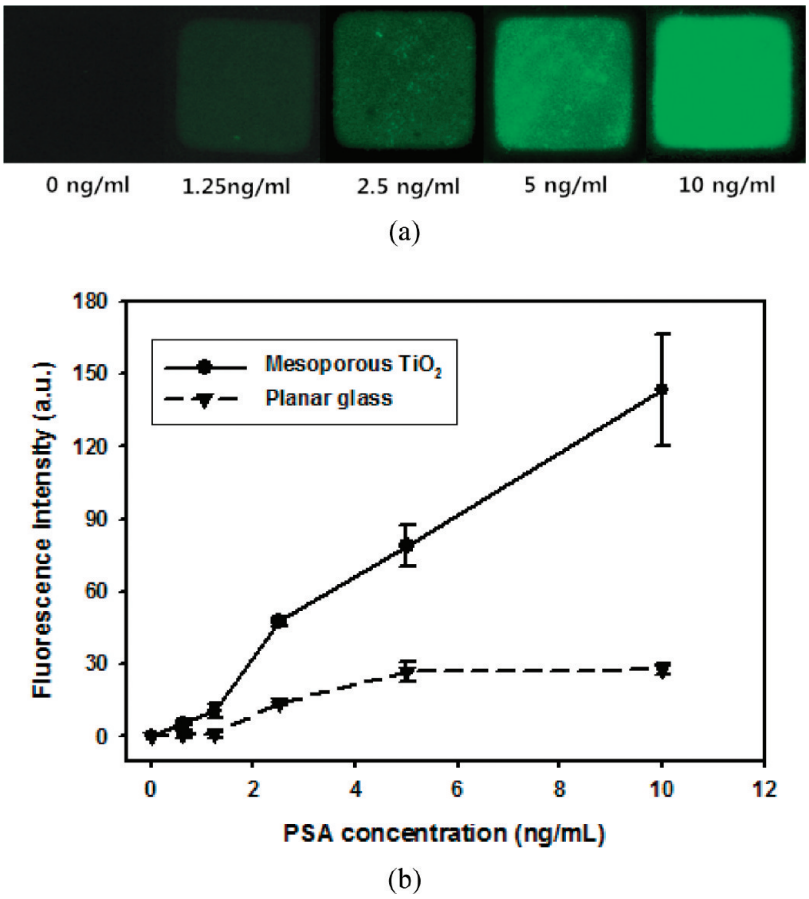

Figure 9. Detection of PSA on micropatterned mesoporous TiO_2 substrate using sandwich immunoassay: (a) fluorescence images of a micropattern that reacted with different concentration of PSA, (b) relationship between concentration of PSA and the fluorescence intensity.

were easily detached from the surfaces in aqueous environments due to swelling of the crosslinked hydrogel matrixes. Therefore, in previous studies, substrate surfaces were usually modified with silane monolayers possessing (meth)arcrylate end-functional groups that participate in photoinitiated free-radical polymerization and covalently anchor hydrogel microstructures to substrates.[34,35] Using relatively thick and interconnected mesoporous TiO_2 as a substrate for hydrogel micropatterning eliminated the necessity of including adhesion-promoting monolayers, because the hydrogel precursor solution was able to infiltrate and crosslink to become securely fixed within pores. Detachment of hydrogel micropatterns from TiO_2 substrates did not occur, even after one month of hydration in water. When silane adhesion promoters with functional (meth)arcrylate groups are used to fabricate hydrogel micropatterns on planar surfaces, it was difficult to covalently immobilize proteins because surface modification agents containing C═C and protein-reactive (e.g., primary amines) functional groups are not commercially available. However, using mesoporous substrates eliminated the need to use silane adhesion promoters, which in turn allowed us to modify TiO_2 substrates for covalent immobilization of proteins.

Microwells consisting of hydrogel walls and mesoporous TiO_2 bottoms were fabricated by photolithography to prepare micropatterned mesoporous substrates for protein microarrays. We fabricated and used microwells with lateral dimensions of 200 × 200 μm (arranged in 20×20 arrays) for protein microarray-based bioassay. SEM images demonstrate the formation of clearly defined hydrogel patterns without residual polymer inside the microwells, preserving the mesoporous structures of TiO_2 substrates (Figure 6). We confirmed that functional groups remained on TiO_2 substrates after UV exposure, probably because 0.2 second UV exposures are too short to induce photocatalysis by TiO_2. Thus, patterning led to clear contrasts between protein-repelling PEG hydrogel regions and glutaraldehyde-activated mesoporous TiO_2 regions. The feasibility of immobilizing proteins on micropatterned mesoporous TiO_2 substrates was investigated by incubating FITC-BSA with micropatterned substrates to visualize the localization and patterning of proteins. Figure 7a shows fluorescence image of micropatterned TiO_2 substrates incubated with FITC-BSA, where fluorescent and dark regions correspond to TiO_2 regions with immobilized BSA and PEG hydrogel regions, respectively. These results indicate that albumin was immobilized only onto TiO_2 micropatterns, with PEG hydrogel serving as an effective barrier to albumin adsorption. Thus, we were able to demonstrate spatial control of protein immobilization on mesoporous TiO_2 substrates on a micrometer scale. Furthermore, Figure 7b indicates that the fluorescence intensities were nearly identical for each microwell, indicating that the amounts of BSA immobilized within different microwells were similar.

Bioassays Using Micropatterned Mesoporous TiO_2 Substrates. To demonstrate the potential use of micropatterned mesoporous TiO_2 substrates in biosensor systems, we first investigated molecular-recognition mediated, specific binding between biotin and streptavidin. The biotin-streptavidin system was chosen for experiments because it provides a universal

platform for patterning a variety of biomolecules. Biotin-NH_2 was covalently immobilized onto the mesoporous bottoms of microwells, and the resultant micropatterned TiO_2 substrates were incubated with a FITC-STV. Fluorescent images demonstrate that streptavidin specifically binds to biotin-immobilized mesoporous TiO_2 microdomains and that nonspecific adsorption was insignificant in the PEG regions (Figure 8a). The fluorescence intensity increased with increasing concentrations of FITC-STV, and the fluorescence intensity and sensitivity (change in signal per change in concentration) was greatly enhanced in mesoporous TiO_2 substrates compared to planar glass slides, as shown in Figure 8b. The detection limits of FITC-STV were 0.01 nM for TiO_2 and 1.0 nM for glass substrates.

After confirming that using mesoporous TiO_2 substrates provides enhanced sensitivity and detection limits compared to conventional glass substrates for use in affinity-based biosensing, we carried out microarray-based immunoassays using mesoporous TiO_2 substrates to detect PSA. PSA is a member of the kallikrein family that is exclusively produced by the prostate gland and has a concentration of 0−4 ng/mL in normal serum.[36] Prostate cancer and other pathological prostatic changes may cause PSA to leak into the peripheral circulation and induce abnormal elevations of serum PSA. PSA concentrations higher than 4 ng/mL may suggest prostate cancer. Fluorescent images shown in Figure 9a reveal that fluorescence-labeled anti-PSA binds only to micropatterned TiO_2 and that fluorescence intensity increases with increased concentrations of PSA. Prior to investigating the relationship between fluorescence intensity and concentrations of PSA, we confirmed that fluorescence signal by non-specific binding were negligible for both substrates and did not affect immunoassay performance. Figure 9b shows the relationship between PSA concentrations and fluorescence intensity for TiO_2 and glass substrate. This figure quantitatively demonstrates that mesoporous TiO_2 substrates can produce higher fluorescence signals and sensitivity than planar glass slides, because 3D mesoporous systems yield increased densities of antibody binding sites and activity. The sensitivity and detection limits of PSA were 14.93 ± 0.81 $(ng/mL)^{-1}$ and 0.62 ng/mL and for TiO_2 substrates, respectively, and 2.42 ± 0.18 $(ng/mL)^{-1}$ and 2.5 ng/mL and for glass slide, respectively. These results demonstrate that micropatterned mesoporous TiO_2 substrates can be used for high-sensitive immunoassays without significant losses of specificity.

CONCLUSION

Protein microarrays were fabricated on multilayered mesoporous TiO_2 substrates for the purpose of improving the sensitivity of immunoassay. A sol−gel process by templating amphiphilic PVC-*g*-POEM graft copolymer produced TiO_2 substrates possessing high-density of interconnected nanosized pores. The surfaces of the TiO_2 substrates were modified to covalently immobilize proteins. The fabrication of nonfouling PEG hydrogel micropatterns on surface-modified TiO_2 substrates allowed us to precisely position proteins only within mesoporous TiO_2 regions. Specific binding assays between streptavidin/biotin and PSA/anti-PSA revealed that mesoporous TiO_2 substrates emitted higher fluorescence signals and were more sensitive with lower detection limits than planar glass substrates, most likely because of the higher protein-loading capacities that resulted from increased surface area. In the future, micropatterned mesoporous substrates can be combined with microprinting systems that locate different proteins into specific microdomains to develop protein microarrays containing different proteins capable of multiplexed protein-based assay.

AUTHOR INFORMATION

Corresponding Author

*E-mail: wongun@yonsei.ac.kr. Phone: 82-2-2123-5755. Fax: 82-2-312-6401.

ACKNOWLEDGMENT

This work was supported by the National Research Foundation (NRF) grant funded by Ministry of Education, Science and Technology (2010K001430 "Converging Research Center Program" and R11-2007-050-03002-0 "Active Polymer Center for Pattern Integration at Yonsei University").

REFERENCES

(1) Zhou, H. H.; Roy, S.; Schulman, H.; Natan, M. J. *Trends Biotechnol.* **2001**, *19*, S34–S39.
(2) MacBeath, G.; Schreiber, S. L. *Science* **2000**, *289*, 1760–1763.
(3) Zhu, H.; Klemic, J. F.; Chang, S.; Bertone, P.; Casamayor, A.; Klemic, K. G.; Smith, D.; Gerstein, M.; Reed, M. A.; Snyder, M. *Nat. Genet.* **2000**, *26*, 283–289.
(4) Hartmann, M.; Roeraade, J.; Stoll, D.; Templin, M.; Joos, T. *Anal. Bioanal. Chem.* **2009**, *393*, 1407–1416.
(5) Templin, M. F.; Stoll, D.; Schwenk, J. M.; Potz, O.; Kramer, S.; Joos, T. O. *Proteomics* **2003**, *3*, 2155–2166.
(6) Angenendt, P. *Drug Disovery Today* **2005**, *10*, 503–511.
(7) Angenendt, P.; Glokler, J.; Sobek, J.; Lehrach, H.; Cahill, D. J. *J. Chromatogr., A* **2003**, *1009*, 97–104.
(8) Barbulovic-Nad, I.; Lucente, M.; Sun, Y.; Zhang, M. J.; Wheeler, A. R.; Bussmann, M. *Crit. Rev. Biotechnol.* **2006**, *26*, 237–259.
(9) Blohm, D. H.; Guiseppi-Elie, A. *Curr. Opin. Biotechnol.* **2001**, *12*, 41–47.
(10) Glokler, J.; Angenendt, P. *J. Chromatogr., B* **2003**, *797*, 229–240.
(11) Kane, R. S.; Takayama, S.; Ostuni, E.; Ingber, D. E.; Whitesides, G. M. *Biomaterials* **1999**, *20*, 2363–2376.
(12) Wilson, D. S.; Nock, S. *Angew. Chem. Int. Ed.* **2003**, *42*, 494–500.
(13) Scopelliti, P. E.; Borgonovo, A.; Indrieri, M.; Giorgetti, L.; Bongiorno, G.; Carbone, R.; Podesta, A.; Milani, P. *PLoS ONE* **2010**, *5*, e11862.
(14) Wang, C.; Zhang, Y.; Seng, H. S.; Ngo, L. L. *Biosens. Bioelectron.* **2006**, *21*, 1638–1643.
(15) Zhang, Y. *Colloid. Surf., B* **2006**, *48*, 95–100.
(16) Son, K. J.; Kim, S.; Kim, J. H.; Jang, W. D.; Lee, Y.; Koh, W. G. *J. Mater. Chem.* **2010**, *20*, 6531–6538.
(17) Ajikumar, P. K.; Kiat, J.; Tang, Y. C.; Lee, J. Y.; Stephanopoulos, G.; Too, H. P. *Langmuir* **2007**, *23*, 5670–5677.
(18) Kang, M. C.; Trofin, L.; Mota, M. O.; Martin, C. R. *Anal. Chem.* **2005**, *77*, 6243–6249.
(19) Stewart, M. P.; Buriak, J. M. *Adv. Mater.* **2000**, *12*, 859–869.
(20) Yang, D. Y.; Liu, X.; Jin, Y.; Zhu, Y.; Zeng, D. D.; Jiang, X. Y.; Ma, H. W. *Biomacromolecules* **2009**, *10*, 3335–3340.
(21) Cao, H. M.; Zhu, Y. H.; Tang, L. H.; Yang, X. L.; Li, C. Z. *Electroanal.* **2008**, *20*, 2223–2228.
(22) Carbone, R.; De Marni, M.; Zanardi, A.; Vinati, S.; Barborini, E.; Fornasari, L.; Milani, P. *Anal. Biochem.* **2009**, *394*, 7–12.
(23) Renault, C.; Balland, V.; Martinez-Ferrero, E.; Nicole, L.; Sanchez, C.; Limoges, B. *Chem. Commun.* **2009**, 7494–7496.
(24) Li, J. L.; Zhao, X. W.; Wei, H. M.; Gu, Z. Z.; Lu, Z. H. *Anal. Chim. Acta* **2008**, *625*, 63–69.
(25) Zhang, Y.; He, P. L.; Hu, N. F. *Electrochim. Acta* **2004**, *49*, 1981–1988.

(26) Song, Y. Y.; Schmidt-Stein, F.; Berger, S.; Schmuki, P. *Small* **2010**, *6*, 1180–1184.
(27) Ahn, S. H.; Koh, J. H.; Seo, J. A.; Kim, J. H. *Chem. Commun.* **2010**, *46*, 1935–1937.
(28) Zhu, H. G.; Srivastava, R.; Brown, J. Q.; McShane, M. J. *Bioconjugate Chem.* **2005**, *16*, 1451–1458.
(29) http://probes.invitrogen.com/media/pis/mp20181.pdf
(30) Cheng, Y. J.; Gutmann, J. S. *J. Am. Chem. Soc.* **2006**, *128*, 4658–4674.
(31) Coakley, K. M.; Liu, Y. X.; McGehee, M. D.; Frindell, K. L.; Stucky, G. D. *Adv. Funct. Mater.* **2003**, *13*, 301–306.
(32) Nedelcu, M.; Lee, J.; Crossland, E. J. W.; Warren, S. C.; Orilall, M. C.; Guldin, S.; Huttner, S.; Ducati, C.; Eder, D.; Wiesner, U.; Steiner, U.; Snaith, H. J. *Soft Matter* **2009**, *5*, 134–139.
(33) Zukalova, M.; Zukal, A.; Kavan, L.; Nazeeruddin, M. K.; Liska, P.; Gratzel, M. *Nano Lett.* **2005**, *5*, 1789–1792.
(34) Revzin, A.; Russell, R. J.; Yadavalli, V. K.; Koh, W. G.; Deister, C.; Hile, D. D.; Mellott, M. B.; Pishko, M. V. *Langmuir* **2001**, *17*, 5440–5447.
(35) Revzin, A.; Tompkins, R. G.; Toner, M. *Langmuir* **2003**, *19*, 9855–9862.
(36) Catalona, W. J.; Hudson, M. A.; Scardino, P. T.; Richie, J. P.; Ahmann, F. R.; Flanigan, R. C.; deKernion, J. B.; Ratliff, T. L.; Kavoussi, L. R.; Dalkin, B. L.; Waters, W. B.; MacFarlane, M. T.; Southwick, P. C. *J. Urol.* **1996**, *155*, 1396–1396.